Electronic Excitations in Single-Wall Carbon Nanotubes: Building-Block Approach

Ralf Hambach[1,3], Christine Giorgetti[1,3], Xochitl Lopez[1,2], and Lucia Reining[1,3].

[1] LSI, Ecole Polytechnique, CNRS-CEA/DSM, Palaiseau, France
[2] University of Texas at San Antonio, United States
[3] European Theoretical Spectroscopy Facility

18. 03. 2011 — DPG Spring Meeting, Dresden

European Theoretical Spectroscopy Facility

Outline

1. Motivation
   - EELS in Carbon Nanotubes
2. Theoretical Approach
   - building-block approach
3. Results
   - $\boldsymbol{q}$-dependence and chirality
   - van-Hove singularities

EELS on SWCNTs

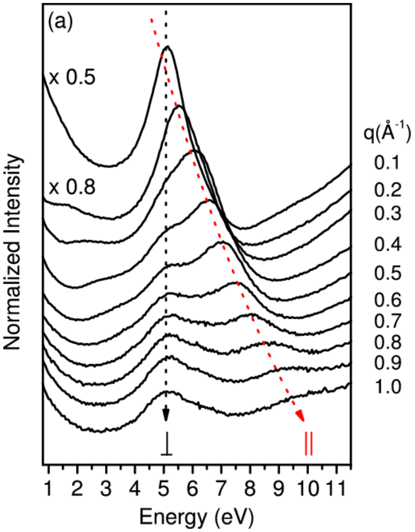

specimen

- oriented SWCNT
- diameter: 2 nm
- nearly isolated

spectroscopy

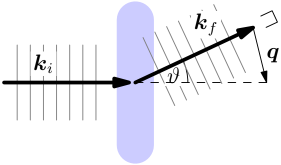

[C. Kramberger, R. H., Ch. Giorgetti, *et.al.*: PRL **101**, 266406 (2008)]

EELS on SWCNTs

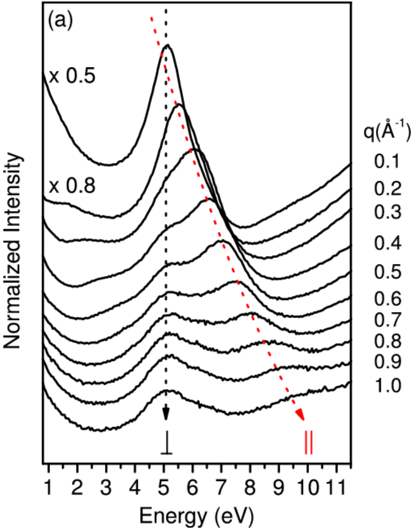

theoretical model

on-axis plasmon in SWCNT ≈ in-plane plasmon in graphene

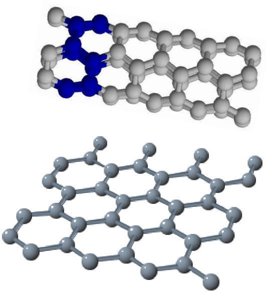

[C. Kramberger, R. H., Ch. Giorgetti, *et.al.*: PRL **101**, 266406 (2008)]

EELS on SWCNTs

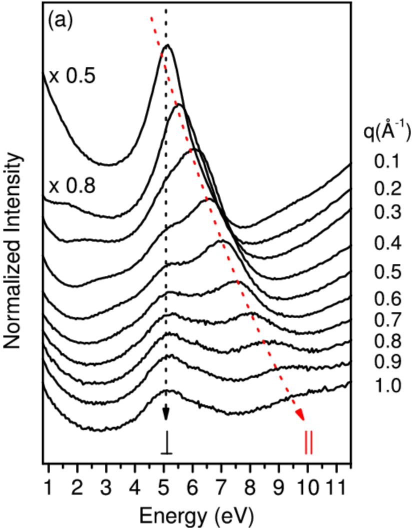

[C. Kramberger, R. H., Ch. Giorgetti, *et.al.*: PRL **101**, 266406 (2008)]

open questions

- How does the spectrum depend on the direction of $\boldsymbol{q}$?
- Is the dispersion given by the modulus $|\boldsymbol{q}|$ or the on-axis component $\boldsymbol{q}_{||}$?
- Is the decomposition of the spectra in perpendicular and parallel contribution valid?

Ab-Initio Calculations

ab initio calculations (DFT, RPA)

1. ground-state calculation gives $\epsilon_\lambda^{\text{KS}}, \varphi_\lambda^{\text{KS}}$
2. Kohn-Sham polarisability χ^0
3. susceptibility $\chi = \chi^0 + \chi^0 v \chi$
4. energy-loss $S(\boldsymbol{q},\omega) = -\frac{1}{\pi}\,\text{Im}\,\chi(\boldsymbol{qq},\omega)$

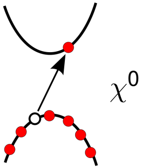

microscopic dielectric response

$$\delta\rho(\boldsymbol{r},t) = \int d\boldsymbol{r}'dt'\; \chi(\boldsymbol{r},\boldsymbol{r}';t-t')\delta V^{ext}(\boldsymbol{r}',t')$$

ABINIT: X. Gonze *et al.*, Comp. Mat. Sci. **25**, 478 (2002)
DP-code: `www.dp-code.org`; V. Olevano, *et al.*, unpublished.

Ab-Initio Calculations

ab initio calculations (DFT, RPA)

1. ground-state calculation gives $\epsilon_\lambda^{\mathrm{KS}}, \varphi_\lambda^{\mathrm{KS}}$
2. Kohn-Sham polarisability χ^0
3. susceptibility $\chi = \chi^0 + \chi^0 v \chi$
4. energy-loss $S(\boldsymbol{q}, \omega) = -\frac{1}{\pi} \operatorname{Im} \chi(\boldsymbol{qq}, \omega)$

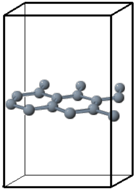

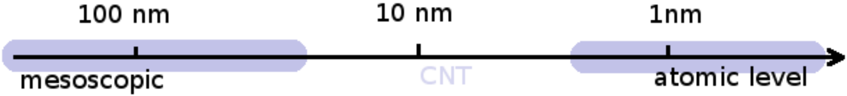

ABINIT: X. Gonze *et al.*, Comp. Mat. Sci. **25**, 478 (2002)
DP-code: `www.dp-code.org`; V. Olevano, *et al.*, unpublished.

Building-Block Approach for SWCNT

full *ab-initio* for periodic graphene ribbon

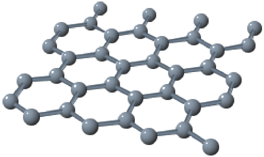

1. ground-state calculation gives ϕ_i^{KS}
2. independent-particle polarisability χ^0_{sheet}

zone-folding model for χ^0

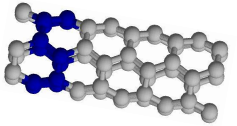

3. polarisability of tube $\chi^0_{\mathrm{sheet}} \to \bar{\chi}^0_{\mathrm{cnt}}$
4. cylinder susceptibility $\bar{\chi} \approx \bar{\chi}^0_{\mathrm{cnt}} + \bar{\chi}^0_{\mathrm{cnt}} v_{\mathrm{cnt}} \bar{\chi}$
5. energy-loss $S = -\frac{1}{\pi} \operatorname{Im} \chi(\boldsymbol{qq}, \omega)$

3. Zone-Folding for Polarisability

cylinder polarisability

$$\bar{\chi}^0_{\text{cnt}}(m, q_z) = R \cdot \chi^0_{\text{sheet}}(q_x, q_y)$$

$\varrho \leftrightarrow R$	radial position
$m/R \leftrightarrow q_x$	azimuthal moment.
$q_z \leftrightarrow q_y$	on-axis momentum

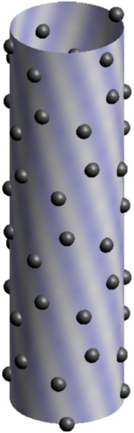

approximations:

- neglect curvature (ZF)

4. Solving the Dyson Equation

cylinder susceptibility

$$\bar{\chi}(m, q_z) \approx \bar{\chi}^0_{\text{cnt}}(m, q_z) + \bar{\chi}^0_{\text{cnt}}(m, q_z)\; v_{\text{cnt}}(m, q_z)\; \bar{\chi}(m, q_z)$$

where $v_{\text{cnt}}(m, q_z) = \frac{e^2}{\varepsilon_0} I_m(|q_z|R)\; K_m(|q_z|R)$ is the Coulomb potential of a cylinder

[M. F. Lin, *et al.*: PRB, 53, 15493 (1996).]

sheet: $\chi = \chi^0 + \chi^0 v \chi$

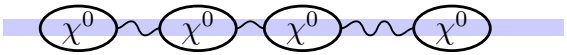

CNT: $\chi = \chi^0 + \chi^0 v_{\text{cnt}} \chi$

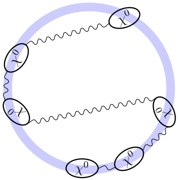

approximations:

- neglect curvature (ZF)
- neglect radial dependence
- homogeneous electron gas

5. AR-EELS for a SWCNT

Response to plane-wave perturbation

- expand external pert. in cylinder waves, $\boldsymbol{q} = (\boldsymbol{q}_\perp, q_z)$:

  $e^{i\boldsymbol{qr}} = e^{iq_\perp \varrho \cos\varphi} e^{iq_z z} = \sum_m i^m J_m(|\boldsymbol{q}_\perp|\varrho)\, e^{im\varphi} e^{iq_z z}$

- susceptibility in Cartesian coord.

  $$\boxed{\chi(\boldsymbol{qq}) = \frac{2\pi}{L^2} \sum_m J_m^2(|\boldsymbol{q}_\perp|R)\, \bar{\chi}(m, q_z)}$$

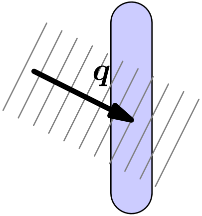

- energy-loss function

  $S(\boldsymbol{q}, \omega) = -\frac{1}{\pi} \operatorname{Im} \chi(\boldsymbol{qq}, \omega)$

Building-Block Approach for SWCNT

full *ab-initio* for periodic graphene ribbon

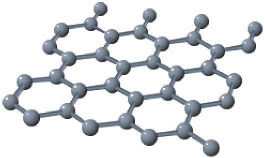

1. ground-state calculation gives ϕ_i^{KS}
2. independent-particle polarisability χ^0_{sheet}

zone-folding model for χ^0

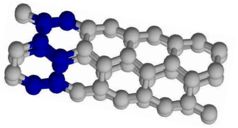

3. polarisability of tube $\chi^0_{\text{sheet}} \to \bar{\chi}^0_{\text{cnt}}$
4. cylinder susceptibility $\bar{\chi} \approx \bar{\chi}^0_{\text{cnt}} + \bar{\chi}^0_{\text{cnt}} v_{\text{cnt}} \bar{\chi}$
5. energy-loss $S = -\frac{1}{\pi}\,\text{Im}\,\chi(\boldsymbol{qq},\omega)$

[Chang, Bussi, Ruini & Molinari: PRL **92**, 196401 (2004)]

Building-Block Approach for SWCNT

full *ab-initio* for periodic graphene ribbon

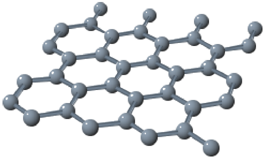

1. ground-state calculation gives ϕ_i^{KS}
2. independent-particle polarisability χ^0_{sheet}

zone-folding model for χ^0

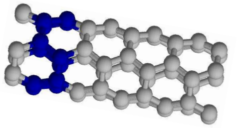

3. polarisability of tube $\chi^0_{\mathrm{sheet}} \to \bar{\chi}^0_{\mathrm{cnt}}$
4. cylinder susceptibility $\bar{\chi} \approx \bar{\chi}^0_{\mathrm{cnt}} + \bar{\chi}^0_{\mathrm{cnt}} v_{\mathrm{cnt}} \bar{\chi}$
5. energy-loss $S = -\frac{1}{\pi}\,\mathrm{Im}\,\chi(\boldsymbol{qq}, \omega)$

$\Longrightarrow$ numerical test for CNT(9,9), [$\oslash$1.2nm]

[Chang, Bussi, Ruini & Molinari: PRL **92**, 196401 (2004)]

Cylinder Response for (9,9) SWCNT

cylinder polarisability $\bar{\chi}^0_{\mathrm{cnt}}(m, q_z)$

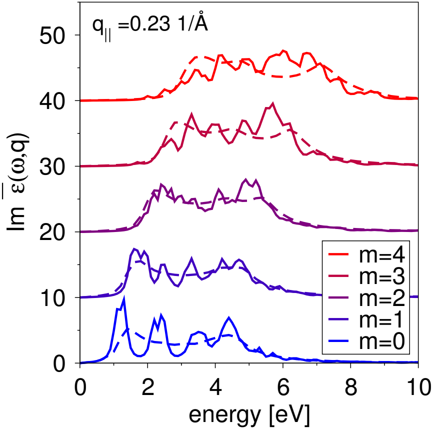

dashed: graphene
solid: graphene ribbon

cylinder susceptibility $\bar{\chi}(m, q_z)$

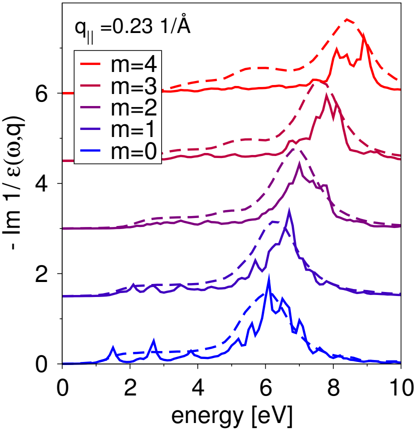

dashed: graphene
solid: graphene ribbon

AR-EELS for CNT(9,9)

EELS for on-axis $q_z = 0.23$ Å^{-1}

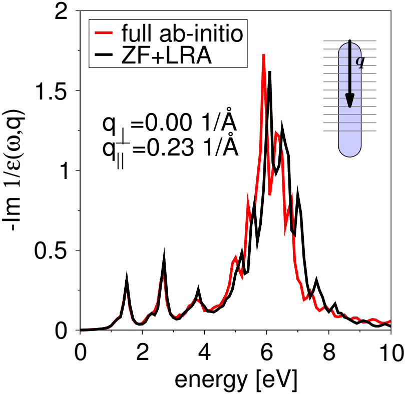

cylinder susceptibility $\bar{\chi}(m, q_z)$

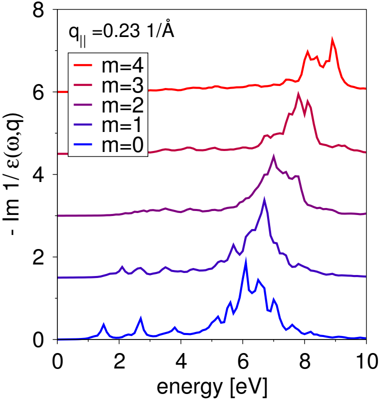

$$\sum_m J_m^2(|\boldsymbol{q}_\perp|R)\ \mathrm{Im}\,\bar{\chi}(m,p)$$

m	0	± 1	± 2	± 3
J_m^2	1	0	0	0

AR-EELS for CNT(9,9)

EELS for off-axis $q = 0.3$ Å^{-1}

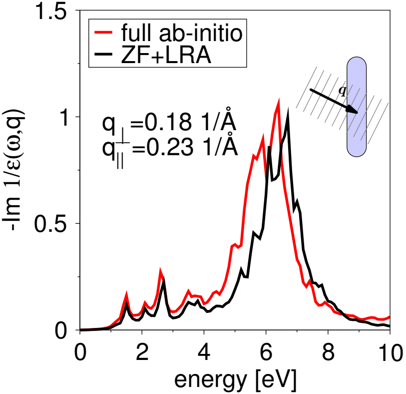

cylinder susceptibility $\bar{\chi}(m, q_z)$

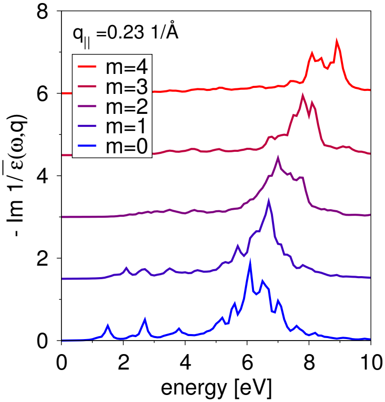

$$\sum_m J_m^2(|\boldsymbol{q}_\perp|R) \;\; \mathrm{Im}\,\bar{\chi}(m, p)$$

m	0	± 1	± 2	± 3
J_m^2	0.5	0.2	0	0

AR-EELS for CNT(9,9)

EELS for off-axis $q = 0.3$ Å^{-1}

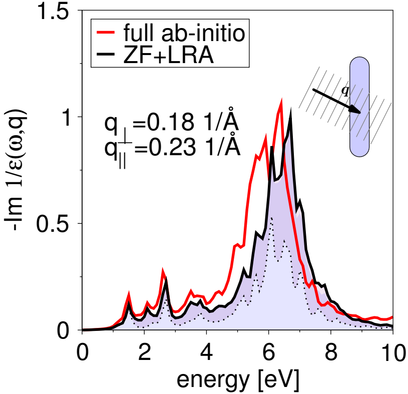

cylinder susceptibility $\bar{\chi}(m, q_z)$

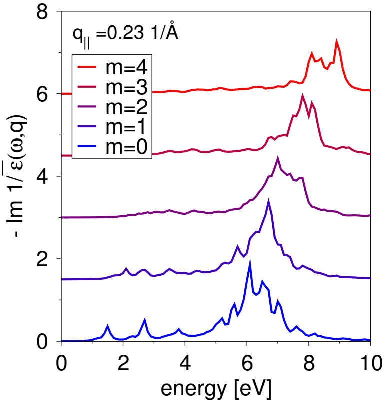

$$\sum_m J_m^2(|\boldsymbol{q}_\perp| R)\ \mathrm{Im}\,\bar{\chi}(m, p)$$

m	0	± 1	± 2	± 3
J_m^2	0.5	0.2	0	0

AR-EELS for CNT(9,9)

EELS for large off-axis $q = 0.9$ Å^{-1}

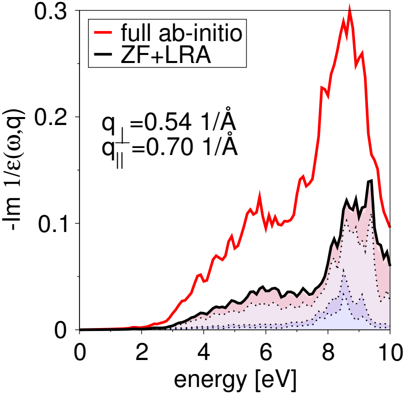

cylinder susceptibility $\bar{\chi}(m, q_z)$

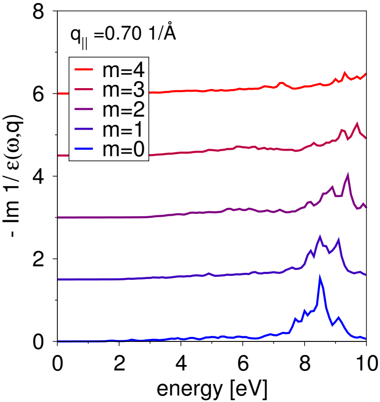

$$\sum_m J_m^2(|\boldsymbol{q}_\perp| R) \;\; \mathrm{Im}\, \bar{\chi}(m, p)$$

m	0	± 1	± 2	± 3
J_m^2	0.1	0.05	0.2	0.1

AR-EELS for CNT(9,9)

EELS for large off-axis $q = 0.9$ Å^{-1}

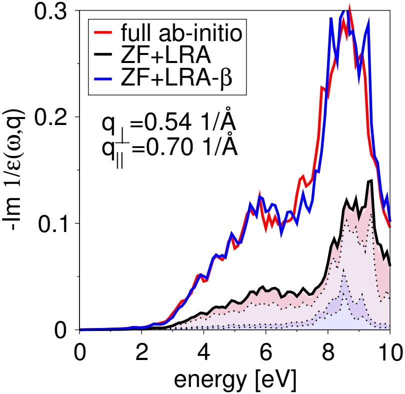

cylinder susceptibility $\bar{\chi}(m, q_z)$

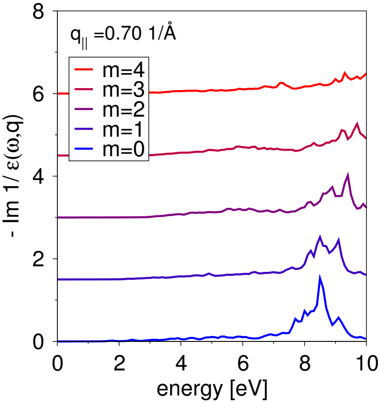

$$\sum_m J_m^2(|\boldsymbol{q}_\perp| R)\ \operatorname{Im} \bar{\chi}(m, p)$$

m	0	± 1	± 2	± 3
J_m^2	0.1	0.05	0.2	0.1

Outline

1. Motivation
   - EELS in Carbon Nanotubes
2. Theoretical Approach
   - building-block approach
3. Results
   - $\boldsymbol{q}$-dependence and chirality
   - van-Hove singularities

Orientation Dependence

(9,9) SWCNT ($\varnothing \approx 12$ Å)

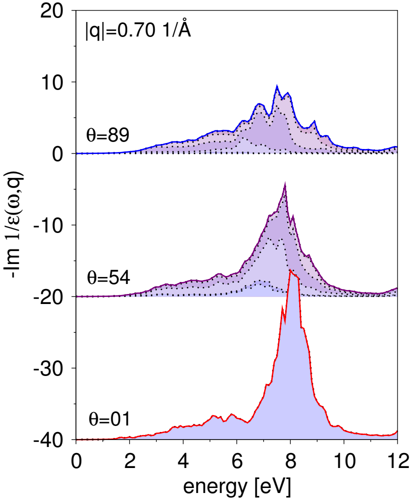

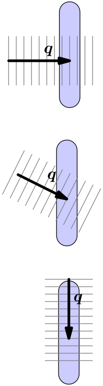

- sum of several m
- broad peak

- only $m = 0$ mode
- sharp peak

Orientation Dependence

(9,9) SWCNT ($\oslash \approx 12$ Å) **(18,18) SWCNT** ($\oslash \approx 24$ Å)

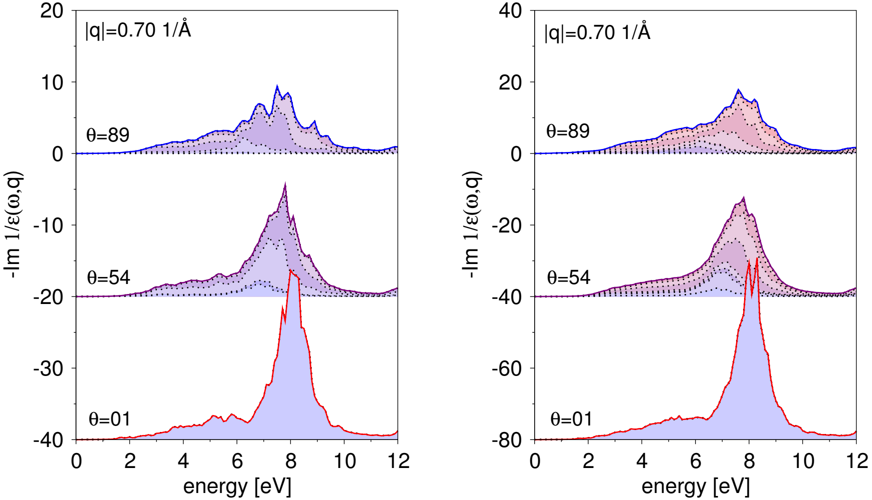

Chirality Dependence

(6,4) SWCNT ($\varnothing \approx 6.8$ Å)

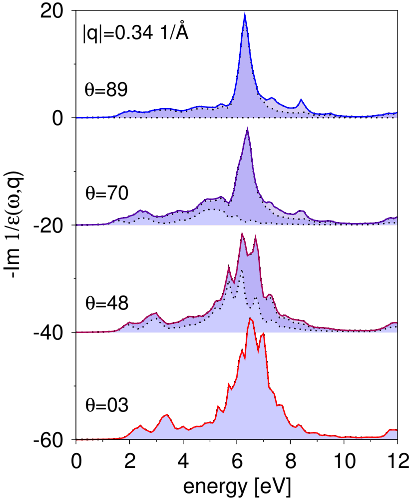

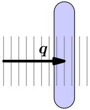

- $m = 1$ dominant
- charact. shape

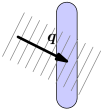

- $m = 0, 1$

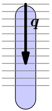

- only $m = 0$ mode
- van-Hove singul.

Chirality Dependence

(6,4) SWCNT ($\oslash \approx 6.8$ Å)

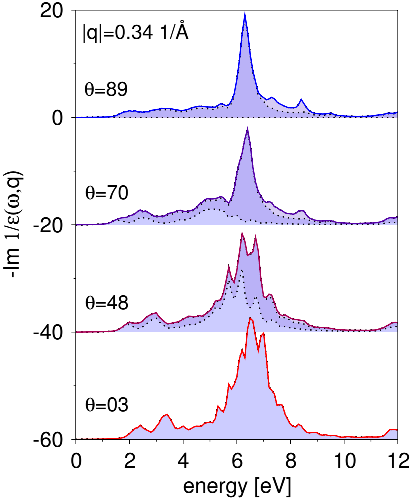

(6,5) SWCNT ($\oslash \approx 7.4$ Å)

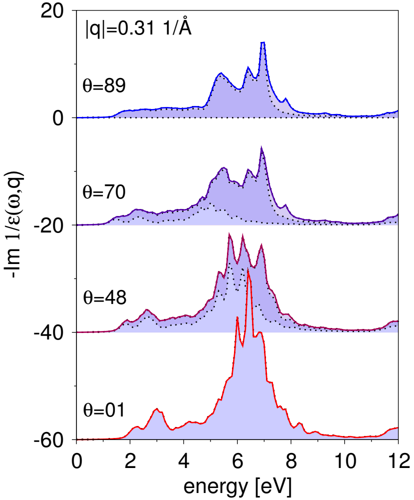

Van-Hove Singularities

(6,4) SWCNT ($\oslash \approx 6.8$ Å)

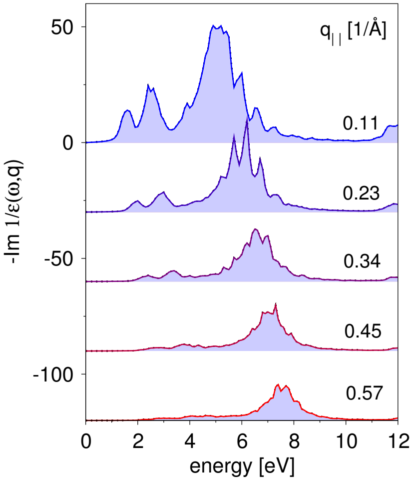

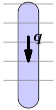

- van-Hove singul.

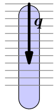

- disperse with $q_{||}$
- vanish for large q

Van-Hove Singularities

(6,4) SWCNT ($\oslash \approx 6.8$ Å)

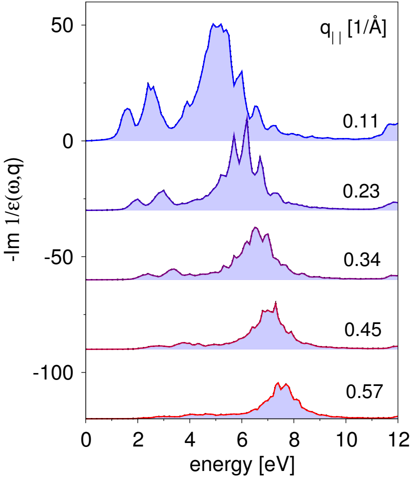

tube polarisability $\bar{\chi}^0_{\text{cnt}}$

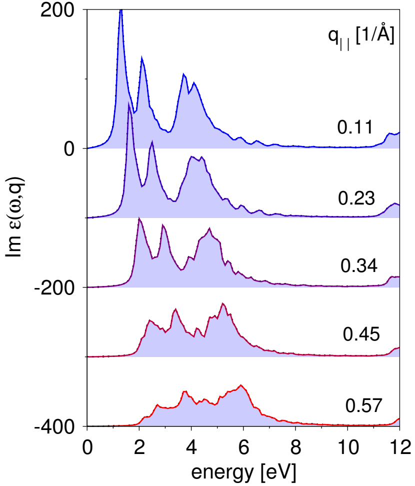

Conclusions

- simple connection graphene $\leftrightarrow$ SWCNTs
- understood AR-EELS in terms of normal-mode excitations
- explained dependence on direction of $\boldsymbol{q}$
- explained dispersion of plasmon peaks

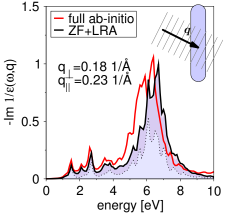

Perspective

- other systems (h-BN, assemblies, doping)
- exchange-correlation effects for $\boldsymbol{q} \to 0$
- different perturbation (SR-EELS)

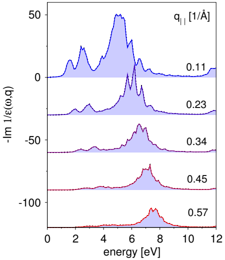

Comparison with Ab-Initio (6x6)

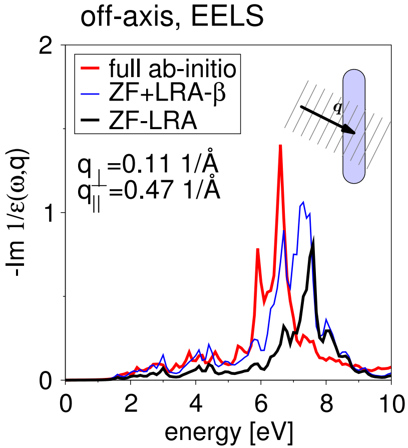

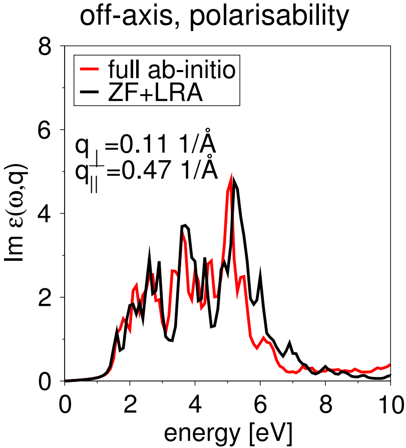

Local-Response Approximation

Dyson equation: coordinates (m, p, ϱ), no in-plane LFE

$$\chi(\varrho, \varrho') = \chi^0(\varrho, \varrho') + \iint d\varrho_1 d\varrho_2\, \varrho_1 \varrho_2\, \chi^0(\varrho, \varrho_1) v(\varrho_1, \varrho_2) \chi(\varrho_2, \varrho')$$

$$v(m, p; \varrho_1 \varrho_2) = \frac{e^2}{\varepsilon_0} I_m(|p|\rho_<)\, K_m(|p|\rho_>)$$

integrated cylinder response functions

$$\bar{\chi}^0(m, p) \equiv \iint d\rho_1 d\rho_2\, \rho_1 \rho_2\, \chi^0(mm, pp; \rho_1 \rho_2)$$

scalar Dyson equation

$$\bar{\chi}(m, p) \approx \bar{\chi}^0(m, p) + \bar{\chi}^0(m, p)\, v_{\text{cnt}}(m, p)\, \bar{\chi}(m, p)$$

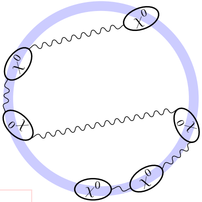

[M. F. Lin, *et al.*: PRB, 53, 15493 (1996).]

Local-Response Approximation

Dyson equation: coordinates (m, p, ϱ), no in-plane LFE

$$\chi(\varrho, \varrho') = \chi^0(\varrho, \varrho') + \iint d\varrho_1 d\varrho_2\, \varrho_1 \varrho_2\, \chi^0(\varrho, \varrho_1) v(R, R) \chi(\varrho_2, \varrho')$$

$$v(m, p; R, R) = \frac{e^2}{\varepsilon_0} I_m(|p|R)\, K_m(|p|R) \equiv v_{\text{cnt}}(m, p)$$

integrated cylinder response functions

$$\bar{\chi}^0(m, p) \equiv \iint d\rho_1 d\rho_2\, \rho_1 \rho_2\, \chi^0(mm, pp; \rho_1 \rho_2)$$

scalar Dyson equation

$$\bar{\chi}(m, p) \approx \bar{\chi}^0(m, p) + \bar{\chi}^0(m, p)\, v_{\text{cnt}}(m, p)\, \bar{\chi}(m, p)$$

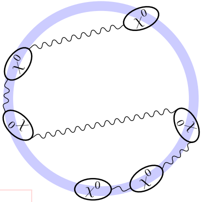

[M. F. Lin, *et al.*: PRB, 53, 15493 (1996).]

Local-Response Approximation

Dyson equation: coordinates (m, p, ϱ), no in-plane LFE

$$\chi(\varrho, \varrho') = \chi^0(\varrho, \varrho') + \iint d\varrho_1 d\varrho_2\, \varrho_1 \varrho_2\, \chi^0(\varrho, \varrho_1) v(R, R) \chi(\varrho_2, \varrho')$$

$$v(m, p; R, R) = \frac{e^2}{\varepsilon_0} I_m(|p|R)\, K_m(|p|R) \equiv v_{\text{cnt}}(m, p)$$

integrated cylinder response functions

$$\bar{\chi}^0(m, p) \equiv \iint d\rho_1 d\rho_2\, \rho_1 \rho_2\, \chi^0(mm, pp; \rho_1 \rho_2)$$

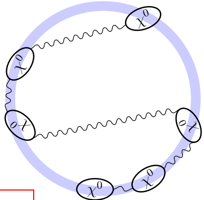

scalar Dyson equation

$$\boxed{\bar{\chi}(m, p) \approx \bar{\chi}^0(m, p) + \bar{\chi}^0(m, p)\, v_{\text{cnt}}(m, p)\, \bar{\chi}(m, p)}$$

[M. F. Lin, *et al.*: PRB, 53, 15493 (1996).]

Dielectric Theory

Local approximation (anisotropic):

$$\epsilon(\omega) = \epsilon_{||}(\omega)\boldsymbol{rr} + \epsilon_{\perp}(\omega)\big(\boldsymbol{zz} + \phi\phi\big)$$

$q_z \leftrightarrow q_x$ on-axis momentum

$m/R \leftrightarrow q_y$ azimuthal momentum

Solution of Dyson equation for:

$$\epsilon^{-1}(m, q_z; \omega) = 1 - \alpha(m, q_z; \omega)$$

$$\alpha(q_z \to \infty; \omega) \propto e^{2q_z R} \left(\frac{\sqrt{\epsilon_\perp \epsilon_{||}} - 1}{\sqrt{\epsilon_\perp \epsilon_{||}} + 1} \right)$$

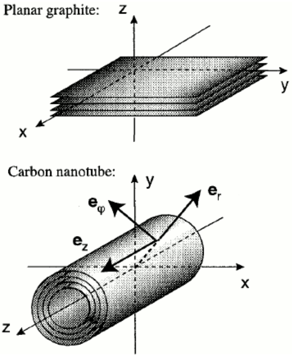

[Taverna,PRB(66),235419 (2002)], [Stöckli, Phil. Mag. B (79), 1531 (1999)]